J|A|C|S
ARTICLES
Published on Web 05/26/2006

Diproline Templates as Folding Nuclei in Designed Peptides. Conformational Analysis of Synthetic Peptide Helices Containing Amino Terminal Pro-Pro Segments

Rajkishor Rai,[†] Subrayashastry Aravinda,[‡] Karuppiah Kanagarajadurai,[†] Srinivasarao Raghothama,[⊥] Narayanaswamy Shamala,*[,‡] and Padmanabhan Balaram*[,†]

Contribution from the Molecular Biophysics Unit, Department of Physics and NMR Research Centre, Indian Institute of Science, Bangalore, 560 012, India

Received February 4, 2006; E-mail: shamala@physics.iisc.ernet.in; pb@mbu.iisc.ernet.in

Abstract: The effect of N-terminal diproline segments in nucleating helical folding in designed peptides has been studied in two model sequences Piv-Pro-Pro-Aib-Leu-Aib-Phe-OMe (**1**) and Boc-Aib-Pro-Pro-Aib-Val-Ala-Phe-OMe (**2**). The structure of **1** in crystals, determined by X-ray diffraction, reveals a helical (α_R) conformation for the segment residues 2 to 5, stabilized by one 4→1 hydrogen bond and two 5→1 interactions. The N-terminus residue, Pro(1) adopts a polyproline II (P_{II}) conformation. NMR studies in three different solvent systems support a conformation similar to that observed in crystals. In the apolar solvent $CDCl_3$, NOE data favor the population of both completely helical and partially unfolded structures. In the former, the Pro-Pro segment adopts an α_R-α_R conformation, whereas in the latter, a P_{II}-α_R structure is established. The conformational equilibrium shifts in favor of the P_{II}-α_R structure in solvents like methanol and DMSO. A significant population of the Pro(1)-Pro(2) *cis* conformer is also observed. The NMR results are consistent with the population of at least three conformational states about Pro-Pro segment: *trans* α_R-α_R, *trans* P_{II}-α_R and *cis* P_{II}-α_R. Of these, the two *trans* conformers are in rapid dynamic exchange on the NMR time scale, whereas the interconversion between *cis* and *trans* form is slow. Similar results are obtained with peptide **2**. Analysis of 462 diproline segments in protein crystal structures reveals 25 examples of the α_R-α_R conformation followed by a helix. Modeling and energy minimization studies suggest that both P_{II}-α_R and α_R-α_R conformations have very similar energies in the model hexapeptide **1**.

Introduction

The template induced folding of peptides is an attractive approach toward the design of engineered sequences with designed secondary structures.[1] In proteins, folding nuclei are formed by small stretches of amino acids, whose local structures are dictated by short-range interactions. The β-turn, a structural feature generated by two residues, is a notable example.[2] Two residue reverse turns, stabilized by 4→1 hydrogen bonds, have been suggesting to be natural templates for nucleating both β-hairpins[3] and helical structures.[4] An isolated β-turn of the type II′ or I′ (prime turn) class is used as a nucleus for inducing a β-hairpin fold in designed synthetic peptides.[5] Two successive type I/III turns generate a single helical turn or an incipient right-handed 3_{10}-helix.[4,6] The conformational requirements for hairpin and helix nucleating turns are distinctly different and are characterized by specific sets of ϕ,ψ torsion angles at the turn residues. Proline is the amino acid with the highest propensity

[†] Molecular Biophysics Unit.
[‡] Department of Physics.
[⊥] NMR Research Centre.

(1) (a) De Grado, W. F. *Adv. Protein Chem.* **1988**, *39*, 51−124. (b) De Grado, W. F.; Raleigh, D. P.; Handel, T. *Curr. Opin. Struct. Biol.* **1991**, *1*, 984−993. (c) Balaram, P. *Curr. Opin. Struct. Biol.* **1992**, *2*, 845−851. (d) Schneider, J. P.; Kelly, J. W. *Chem. Rev.* **1995**, *95*, 2169−2187. (e) Tuchscherer, G.; Grell, D.; Mathieu, M.; Mutter, M. *J. Peptide Res.* **1999**, *54*, 185−194. (f) Venkatraman, J.; Shankaramma, S. C.; Balaram, P. *Chem. Rev.* **2001**, *101*, 3131−3152.

(2) (a) Venkatachalam, C. M. *Biopolymers* **1968**, *6*, 1425−1436. (b) Rose, G. D.; Gierasch, L. M.; Smith, J. A. *Adv. Protein Chem.* **1985**, *37*, 1−109. (c) Richardson, J. S.; Richardson, D. C. In *Prediction of Protein Structure and the principles of Protein Conformation*; Fasman, G. D., Ed.; Plenum Press: New York, 1989; pp 1−98.

(3) (a) Sibanda, B. L.; Thornton, J. M. *Nature* **1985**, *316*, 170−174. (b) Sibanda, B. L.; Blundell, T. L.; Thornton, J. M. *J. Mol. Biol.* **1989**, *206*, 759−777. (c) Hutchinson, E. G.; Thornton, J. M. *Protein Sci.* **1994**, *3*, 2207−2216. (d) Gunasekaran, K.; Ramakrishnan, C.; Balaram, P. *Protein Eng.* **1997**, *10*, 1131−1141.

(4) Venkatachalapathi, Y. V.; Balaram, P. *Nature* **1979**, *281*, 83−84.

(5) For reviews see: (a) Balaram, P. *Proc. Ind. Acad. Sci. (Chem. Sci.)* **1984**, *93*, 703−717. (b) Gellman, S. H. *Curr. Opin. Chem. Biol.* **1998**, *6*, 717−725. (c) Balaram, P. *J. Peptide Res.* **1999**, *54*, 195−199. (d) Kaul, R. K.; Balaram, P. *Bioorg. Med. Chem.* **1999**, *7*, 105−117. (e) Two residue turns in polypeptide structures are conventionally classified on the basis of the Ramachandran torsion angles at the turn residues denoted as $i+1$ and $i+2$. Two major turn types have been identified: type I/III ($\phi_{i+1} = -60°$, $\psi_{i+1} = -30°$, $\phi_{i+2} = -90°$, $\psi_{i+2} = 0°$ for type I and $\phi_{i+1} = -60°$, $\psi_{i+1} = -30°$, $\phi_{i+2} = -60°$, $\psi_{i+2} = -30°$ for type III) and type II ($\phi_{i+1} = -60°$, $\psi_{i+1} = 120°$, $\phi_{i+2} = 80°$, $\psi_{i+2} = 0°$). The enantiomeric ("prime" turns) type I′/III′ and II′ are obtained by inverting the sign of the torsion angles. Type I and III turns need not be considered separately as they are structurally similar. The key difference between type I and Type II turn is the orientation of the central peptide unit, the amide bond between residues $i+1$ and $i+2$, which under goes a flip during a type I−type II transition. (Gunasekaran, K.; Gomathi, L.; Ramakrishnan, C.; Chandrasekhar, J.; Balaram, P. *J. Mol. Biol.* **1998**, *284*, 1505−1516). (f) The term "folding nucleus" is often used implicitly assuming that formation of the short-range structural feature (example β-turn) precedes the generation of the larger structural elements (helix or hairpin). Most studies in the area of designed peptides examine the final folded structure and thus provide no direct evidence for the kinetic pathway of folding.

10.1021/ja060674v CCC: $33.50 © 2006 American Chemical Society

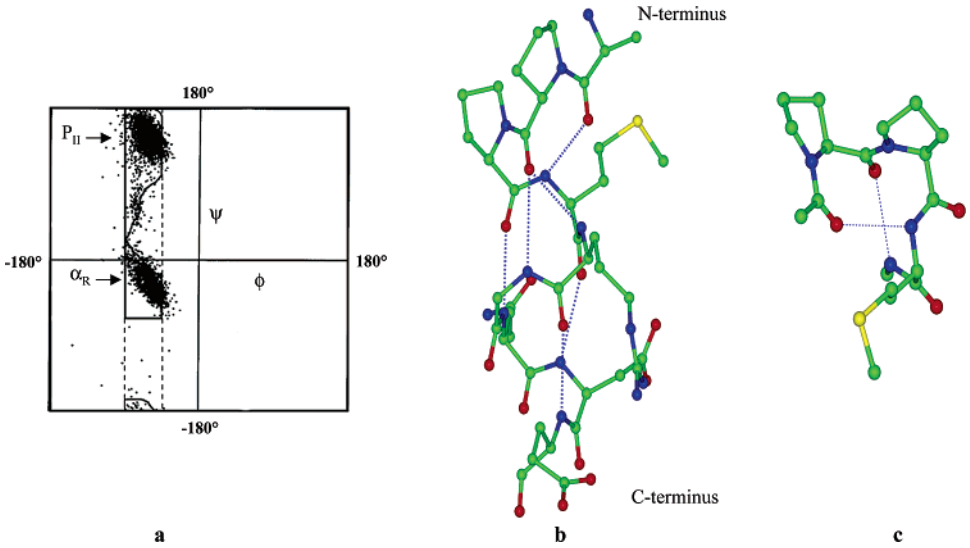

Figure 1. (a) Allowed regions in Ramachandran space for ^{L}Pro residues. Note that the torsion angle ϕ is restricted to a relatively narrow range of ϕ values, ^{L}Pro = $-60 \pm 20°$.[1f] Observed distribution of conformational angles for 4995 Pro residues in 538 protein crystal structures.[47] (b) An example of a diproline segment from the protein gingipain-R (PDB code: 1CVR)[9] that adopts the α_R-α_R conformation. (c) Expanded view of the diproline segment highlighting the stabilization of the consecutive β-turn conformation by two 4→1 hydrogen bonds.

to occur in turn structures in proteins,[2c,7] because of the constraints of pyrrolidine ring formation, which lock the ϕ value for ^{L}Pro to $\sim -60° \pm 20°$ (Figure 1a). Analyses of helices in protein structures reveal that Pro has a high propensity to occur in the N-cap regions (amino terminus end) because of a favorable ϕ value, which lies in the region expected for helices, and the absence of hydrogen bonding interactions involving the NH groups of the first two or three residues of polypeptide helices.[8] Figure 1b illustrates an example of a helical segment in a protein structure, in which the diproline unit occurs at the amino terminus. The Pro-Pro segment forms a turn of a helical structure, stabilized by two successive intramolecular 4→1 hydrogen bonds (Figure 1c).[9] An inversion of the configuration of the N-terminal proline residue results in a variant of the consecutive β-turn structure, in which a type II′ ^{D}Pro-^{L}Pro turn is followed by a type I/III ^{L}Pro-^{L}Xxx turn (Figure 2a).[10] In principle, a II′-I/III consecutive turn (or its enantiomer II−I′/III′) structure also serves to propagate a helical fold, as exemplified in the structure of synthetic model peptides. In this case, the II′-I consecutive turn nucleates a *right-handed* helix (α_R), whereas the enantiomeric structure (II−I′) facilitates formation of a *left-handed* helix (α_L) (Figure 2b).[11] In contrast, an isolated type II′ β-turn formed by ^{D}Pro-^{L}Pro segments may be employed as an effective hairpin nucleator in both cyclic and acyclic peptides.[12] While heterochiral ^{D}Pro-Xxx and ^{D}Pro-^{L}Pro segments have been demonstrated to be very effective hairpin nucleators in many recent studies,[13] relatively few investigations have focused on the role of the homochiral diproline segment in nucleating helices.

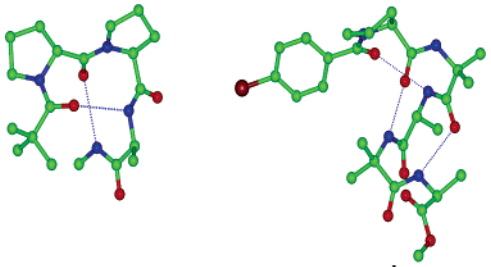

Figure 2. Solid-state conformation of (a) Piv-^{D}Pro-^{L}Pro-^{L}Ala-NHMe (type II′-I consecutive β-turn).[10] (b) *p*-chlorobenzyl-^{L}Pro-Aib-^{L}Ala-Aib-^{L}Ala-OMe (type II−I′ consecutive β-turn).[11]

An early suggestion that diproline segments could serve to nucleate helical folding was based on the conformational

(6) (a) Shamala, N.; Nagaraj, R.; Balaram, P. *Biochem. Biophys. Res. Commun.* **1977**, *79*, 291−298. (b) Nagaraj, R.; Shamala, N.; Balaram, P. *J. Am. Chem. Soc.* **1979**, *101*, 16−20.
(7) (a) Chou, P. Y.; Fasman, G. D. *J. Mol. Biol.* **1977**, *115*, 135−175. (b) Wilmot, C. M.; Thornton, J. M. *J. Mol. Biol.* **1988**, *203*, 221−232.
(8) (a) Presta, T. L.; Rose, G. D. *Science* **1988**, *240*, 1632−1641. (b) Richardson, J. S.; Richardson, D. C. *Science* **1988**, *240*, 1648−1652. (c) Aurora, R.; Rose, G. D. *Protein Sci.* **1998**, *7*, 21−38. (d) Gunasekaran, K.; Nagarajaram, H. A.; Ramakrishnan, C.; Balaram, P. *J. Mol. Biol.* **1998**, *275*, 917−932. (e) Viguera, A. R.; Serrano, L. *Protein Sci.* **1999**, *8*, 1733−1742.
(9) Eichinger, A.; Beisel, H. G.; Jacob, U.; Huber, R.; Medrano, F. J.; Banbula, A.; Potempa, J.; Travis, J.; Bode, W. *EMBO J.* **1999**, *18*, 5453−5462.
(10) Nair, C. M. K.; Vijayan, M.; Venkatachalapathi, Y. V.; Balaram, P. *J. Chem. Soc., Chem. Commun.* **1979**, 1183−1184.
(11) (a) Cameron, T. S. *Cryst. Struct. Comm.* **1982**, *11*, 321−330. (b) Prasad, B. V. V.; Balaram, P. In *Conformation in Biology*; Srinivasan, R., Sarma, R. H., Eds.; Adenine Press: New York, pp 133−140, 1982. (c) Prasad, B. V. V.; Balaram, P. *CRC Crit. Rev. Biochem.* **1984**, *16*, 307−348.
(12) (a) Robinson, J. A. *Synlett.* **2000**, *4*, 429−441. (b) Shankaramma, S. C.; Athanassiou, Z.; Zerbe, O.; Moehle, K.; Mouton, C.; Bernardini, F.; Vrijbloed, J. W.; Obrecht, D.; Robinson, J. A. *Chembiochem* **2002**, *3*, 1126−1133. (c) Robinson, J. A.; Shankaramma, S. C.; Jetter, P.; Kienzl, U.; Schwendener, R. A.; Vrijbloed, J. W.; Obrecht, D. *Bioorg. Med. Chem.* **2005**, *13*, 2055−2064. (d) Hanessian, S.; Angiolini, M. *Chem.—Eur. J.* **2002**, *8*, 111−117. (e) Rai, R.; Raghothama, S.; Balaram, P. *J. Am. Chem. Soc.* **2006**, *128*, 2675−2681. (f) In ongoing work from this laboratory a β-hairpin structure has been characterized by X-ray diffraction in crystals of the peptide Boc-Leu-Phe-Val-^{D}Pro-^{L}Pro-Leu-Phe-Val-OMe (unpublished).
(13) (a) Awasthi, S. K.; Raghothama, S.; Balaram, P. *Biochem. Biophys. Res. Commun.* **1995**, *216*, 375−381. (b) Karle, I. L.; Awasthi, S. K.; Balaram, P. *Proc. Natl. Acad. Sci. U.S.A.* **1996**, *93*, 8189−8193. (c) Haque, T. S.; Little, J. C.; Gellman, S. H. *J. Am. Chem. Soc.* **1996**, *118*, 6975−6985. (d) Haque, T. S.; Gellman, S. H. *J. Am. Chem. Soc.* **1997**, *119*, 2303−2304. (e) Raghothama, S. R.; Awasthi, S. K.; Balaram, P. *J. Chem. Soc., Perkin Trans 2.* **1998**, 137−143. (f) Espinosa, J. F.; Gellman, S. H. *Angew. Chem., Int. Ed.* **2000**, *39*, 2330−2333. (g) Karle, I. L.; Gopi, H. N.; Balaram, P. *Proc. Natl. Acad. Sci. U.S.A.* **2001**, *98*, 3716−3719. (h) Karle, I. L.; Gopi, H. N.; Balaram, P. *Proc. Natl. Acad. Sci. U.S.A.* **2002**, *99*, 5160−5164. (i) Aravinda, S.; Harini, V. V.; Shamala, N.; Das, C.; Balaram, P. *Biochemistry* **2004**, *43*, 1832−1846. (j) Harini, V. V.; Aravinda, S.; Rai, R.; Shamala, N.; Balaram, P. *Chem.—Eur. J.* **2005**, *11*, 3609−3620. (k) Lamm, M. S.; Rajagopal, K.; Schneider, J. P.; Pochan, D. J. *J. Am. Chem. Soc.* **2005**, *127*, 16692−16700. (l) Haines, L. A.; Rajagopal, K.; Ozbas, B.; Salick, D. A.; Pochan, D. J.; Schneider, J. P. *J. Am. Chem. Soc.* **2005**, *127*, 17025−17029.

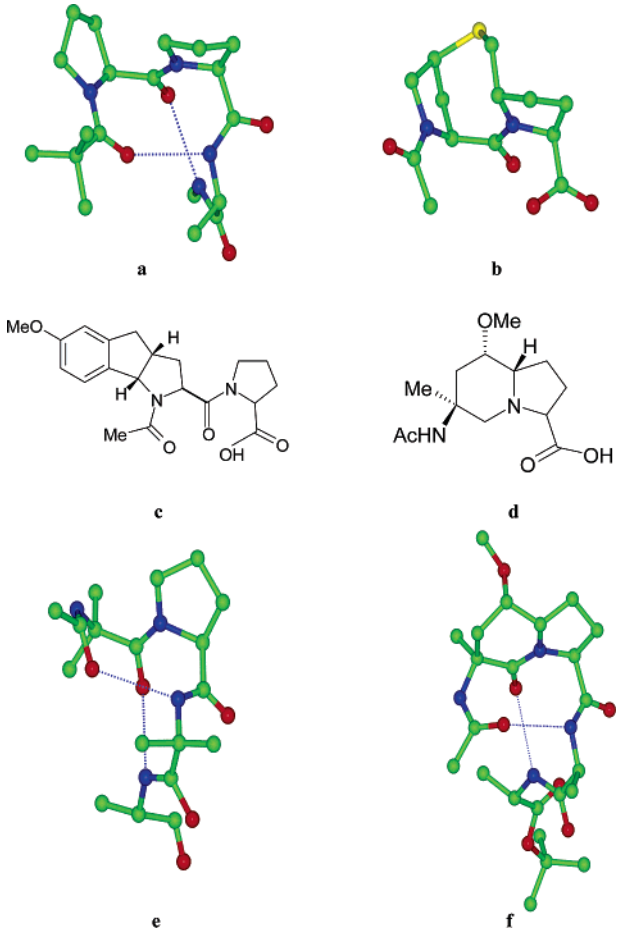

Figure 3. Templates, used to nucleate helical structures. (a) NMR model of Piv-^{L}Pro-^{L}Pro-^{L}Ala-NHMe.[4] (b) Structure of Kemp's template (2*S*,5*S*,8*S*,-11*S*)-1-acetyl-1,4-diaza-3-keto-5-carboxy-10-thiatricyclo [2.8.1.0^{4,8}]-tridecane (Ac−Hel$_1$−OH) in crystals.[14c] (c) Ac-^{L}TcaP-^{L}Pro-OH. (TcaP = tricyclic constrained proline).[16a] (d) (3S,6S,8S,9S)-6-acetylamino-8-methoxy-6-methyl-5-oxooctahydroindolizine-3-carboxylic acid (^{L}BcaP).[16a] (e) Crystal structure of the alamethicin segment Ac-Aib-Pro-Aib-Ala.[49] (f) Crystal structure of ^{L}BcaP-^{L}Ala-^{L}Ala-OtBu.[16a,50]

analysis of the model peptide Piv-^{L}Pro-^{L}Pro-^{L}Ala-NHMe, in which the observation of two intramolecular hydrogen bonds was interpreted in favor of an incipient 3_{10}-helical structure (Figure 3a).[4] Subsequently, synthetic templates based on diproline structures have been devised and shown to strongly promote helical folding when positioned at the N-terminus of synthetic sequences. In a series of elegant studies, Kemp and co-workers established the helix nucleating properties of synthetic templates based on a bicyclic, diproline mimetic scaffold.[14] Kemp's scaffold may be viewed as a tricyclic analogue of the diproline segment, in which the C$^{\gamma}$ atom of Pro(1) and C$^{\delta}$ atom of Pro-(2) are bridged by a thiomethylene group (Figure 3b). This constraint effectively limits excursions of the Pro(1) ψ torsion angle and orients the first two carbonyl groups in the same direction, a feature that promotes helical hydrogen bond formation as the chain lengthens. A bicyclic hexahydroindene-4-one 3,6-diacid has also been shown to be an effective inducer of helix formation in appended peptides.[15] More recently, Hanessian and co-workers have reported two helix-inducing templates, a bicyclic indolizidinone carboxylic acid and a tricyclic proline derivative, which have been used as the N-terminus residue in short Ala rich peptides (Figure 3).[16] The Hanessian template shown in Figure 3d is formally equivalent to the Aib-Pro unit, which is known to nucleate a local 3_{10}-helical fold.[6,11b,c]

There are, as yet, no examples of synthetic peptide helices in which the native diproline segment is placed at the amino terminus. As a part of program to systematically explore the context dependent conformation of diproline segments, we describe structural studies on the model peptides Piv-Pro-Pro-Aib-Leu-Aib-Phe-OMe (**1**) and Boc-Aib-Pro-Pro-Aib-Val-Ala-Phe-OMe (**2**). The choice of the sequence is based on the well-established ability of Aib residues to promote helical folding in short peptides,[6,11c,17] with the specific intention of probing whether continuous helix formation can be demonstrated over the entire length of the peptide. The C-terminus stretch of apolar residues was intended to promote solubility in poorly solvating media like chloroform, which may be expected to support intramolecularly hydrogen bonded structures, by eliminating solvent competition for donor and acceptor sites on the peptide backbone. The use of the bulky Piv group for blocking the N-terminus of Pro(1) precludes the formation of the *cis* conformer about the X-Pro(1) bond.[4,18] Studies of proline containing peptides need to consider the formation of *cis* conformations about the X-Pro tertiary amide bond.[19] The Aib residue is sterically analogous to the pivaloyl group eliminating the possibility of *cis* Aib-Pro(1) conformations in peptides.[20] The results described in this report establish that in peptide **1** Pro(2) occurs at the N-terminus of the helix adopting a local α_R conformation, while Pro(1) adopts a semi- extended, polyproline (P_{II}) conformation in the solid state. In solution, NMR evidence suggests that peptide **1** exists as a mixture of *trans* and *cis* Pro-Pro conformers, with the former being largely predominant. The *trans* Pro-Pro form exists as an equilibrium mixture of the continuous helix and the partially unfolded helix in $CDCl_3$ solution. In polar solvents, the equilibrium shifts in favor of the conformer characterized in crystals. In peptide **2**, the amino terminus segment favors a folded, intramolecularly hydrogen bonded conformation in both *cis* and *trans* Pro-Pro conformers.

Experimental Section

Peptide Synthesis. Peptides **1** and **2** were synthesized by conventional solution phase methods using a fragment condensation strategy. The pivaloyl (Piv) and *tert*-butyloxycarbonyl (Boc) groups were used for the N-terminus, while the C-terminus was protected as a methyl

(14) (a) Kemp, D. S.; Boyd, J. G.; Muendel, C. C. *Nature* **1991**, *352*, 451−454. (b) Kemp, D. S.; Curran, T. P.; Boyd, J. G.; Allen, T. J. *J. Org. Chem.* **1991**, *56*, 6683−6697. (c) Kemp, D. S.; Curran, T. P.; Davis, W. M.; Boyd, J. G.; Muendel, C. *J. Org. Chem.* **1991**, *56*, 6672−6682. (d) Job, G. E.; Heitmann, B.; Kennedy, R. J.; Walker, S. M.; Kemp, D. S. *Angew. Chem., Int. Ed.* **2004**, *43*, 5649−5651. (e) Heitmann, B.; Job, G. E.; Kennedy, R. J.; Walker, S. M.; Kemp, D. S. *J. Am. Chem. Soc.* **2005**, *127*, 1690−1704.

(15) Austin, R. E.; Maplestone, R. A.; Sefler, A. M.; Liu, K.; Hruzewicz, W. N.; Liu, C. W.; Cho, H. S.; Wemmer, D. E.; Bartlett, P. A. *J. Am. Chem. Soc.* **1997**, *119*, 6461−6472.

(16) (a) Hanessian, S.; Papeo, G.; Fettis, K.; Therrien, E.; Viet, M. T. *J. Org. Chem.* **2004**, *69*, 4891−4899. (b) Hanessian, S.; Papeo, G.; Angiolini, M.; Fettis, K.; Beretta, M.; Munro, A. *J. Org. Chem.* **2003**, *68*, 7204−7218. (c) Hanessian, S.; Sailes, H.; Munro, A.; Therrien, E. *J. Org. Chem.* **2003**, *68*, 7219−7233.

(17) (a) Toniolo, C.; Benedetti, E. *ISI Atlas of Science: Biochemistry* **1988**, *1*, 225−230. (b) Karle, I. L.; Balaram, P. *Biochemistry* **1990**, *29*, 6747−6756. (c) Toniolo, C.; Benedetti, E. *Trends Biochem. Sci.* **1991**, *16*, 350−353.

(18) Nishihara, H.; Nishihara, K.; Uefuji, T.; Sakota, N. *Bull. Chem.* Soc. *Jpn.* **1975**, *48*, 553−555.

(19) (a) Gratwohl, C.; Wüthrich, K. *Biopolymers* **1976**, *15*, 2025−2041. (b) Ramachandran, G, N.; Mitra, A. K. *J. Mol. Biol.* **1976**, *107*, 85−92.

(20) Balaram, H.; Prasad, B. V. V.; Balaram, P. *J. Am. Chem. Soc.* **1983**, *105*, 4065−4071.

ester. Deprotections were performed using 98% formic acid and saponification for the N- and C-terminal protection groups, respectively. Couplings were mediated by dicyclohexylcarbodiimide/1-hydroxybenzotriazole (DCC/HOBT).[21] All the intermediates were characterized by ^{1}H NMR (80 MHz) and TLC (silica gel, 9:1 chloroform-methanol), and were used without further purification. The final peptides were purified by medium-pressure liquid chromatography (MPLC) on a C_{18} column (40−60 μ) followed by HPLC (C_{18}, 5−10 μ), employing methanol−water gradients. The homogeneity of the purified peptides was ascertained by analytical HPLC. The purified peptides were characterized by electrospray ionization mass spectrometry (ESI−MS), and by complete assignment of the 500 MHz NMR spectra. (ESI−MS: $M_{cal} = 740$; $M_{obs} = 763$ Da [M + Na$^+$] for peptide **1** and $M_{cal} = 813$; $M_{obs} = 836$ Da [M + Na$^+$] for peptide **2**).

X-ray Diffraction. Crystals of peptide **1** were grown by slow evaporation of methanol/water/DMSO mixtures. The X-ray data were collected on a Bruker AXS SMART APEX CCD diffractometer, using Mo Kα radiation ($\lambda = 0.710\ 73$ Å). ω scan type was used, with $2\theta = 53°$, for a total of 8383 unique reflections. The crystal size was $0.58 \times 0.28 \times 0.17$ mm. The space group is $P2_1$ with $a = 13.910(1)$ Å, $b = 19.766(2)$ Å, $c = 15.762(1)$ Å, $\beta = 98.03°$, $V = 4291.0(6)$ Å^3, $Z = 4$ for chemical formula $C_{39}H_{60}N_6O_8$, with two molecule per asymmetric unit. $\rho_{calc} = 1.15$ g cm^{-3}, $\mu = 0.08$ mm^{-1}, $F(000) = 1600$. The structure was obtained by direct methods using SHELXD.[22a] Refinement was carried out against F^2, with full matrix least-squares methods using SHELXL-97.[22b] All non-hydrogen atoms were refined isotropically. The R value at the end of isotropic refinement was 0.146. The R value dropped to 0.084 after anisotropic refinement. The hydrogen atoms were fixed geometrically in idealized positions and refined in the final cycle of refinement as riding over the atoms to which they are bonded. The final R value was 0.0546 ($wR_2 = 0.145$) for observed reflections 6406 with $F_0 \geq 4\sigma(|F_0|)$ and 955 variables, where the data-to-parameter ratio is 6.7:1.0 and $S = 1.081$. The largest difference peak was 0.45 e/Å^3 and the largest difference hole was −0.18 e/Å^3.

NMR. NMR experiments were carried out on a Bruker DRX500 spectrometer. 1D and 2D spectra were recorded at a peptide concentration of ~3 mM in $CDCl_3$, CD_3OH and DMSO-d_6 at 300 K. Delineation of exposed NH groups was achieved by titrating a $CDCl_3$ solution with low concentrations of DMSO-d_6. In the case of CD_3OH and DMSO-d_6, intramolecular hydrogen bonding was probed by recording 1D spectra at 5 different temperatures between 275−323 K at 10° intervals and determining the temperature coefficients of amide proton chemical shifts.

Resonance assignments were carried out with the help of 1D and 2D spectra. Residue specific assignments were obtained from TOCSY[23] experiments while NOESY/ROESY[24] spectra permitted sequence specific assignments. All 2D experiments were recorded in phase sensitive mode using the TPPI (time proportional phase incrementation) method. A data set of 1024×450 was used for acquiring the data. The same data set was zero filled to yield a data matrix of size 2048×1024 before Fourier transformation. A spectral width of 6000 Hz was used in both dimensions. Mixing times of 100 and 200 ms were used for TOCSY and ROESY, respectively. Shifted square sine bell windows were used while processing. All processing was done using BRUKER XWINNMR software.

Analysis of Pro-Pro Segments in Proteins. The data set was retrieved from the pre-compiled culled database of protein structures prepared by R. L. Dunbrack and G. L. Wang.[25] The data set used in the present study was further filtered using a resolution cutoff ≤2.0 Å, sequence similarity cutoff ≤20% and R-factor limit 0.25. A total of 1741 protein chains were obtained, which include only nonredundant sequences in each pdb file.[26] The following pattern X-X-X-P-P-X-X-X (where X is any amino acid except proline) was searched using the above database through Expasy scan prosite.[27] A total of 462 diproline units from 372 independent chains (366 unique proteins) were identified. The diproline segments were classified into four distinct groups, *cis-cis*, *cis-trans*, *trans-cis*, *trans-trans* (*cis* $\omega \approx 0°$; *trans* $\omega \approx 180°$). These were further subdivided into six conformational categories based on ϕ,ψ values. α-α, α-P_{II}, P_{II}-α, P_{II}-P_{II}, P_{II}-bridge, others. The following limits have been used for definition of the regions of ϕ,ψ space: α, $\phi = -30°$ to $-90°$, $\psi = -30°$ to $-60°$; P_{II}, $\phi = -30°$ to $-100°$, $\psi = 100°$ to 180°.

Results and Discussion

Molecular Conformation of 1 in Crystals. Peptide **1** crystallized with two independent molecules in the crystallographic asymmetric unit. Figure 4 illustrates the observed conformation of the molecule, while Tables 1 and S1(Supporting Information) list the backbone and side chain torsion angles and the inter- and intramolecular hydrogen bond parameters, respectively. Both the molecules adopt very similar conformations; superposition yields an RMS deviation for all backbone atoms of 0.124 Å. The backbone torsion angles for residues 2 to 5 lie in the helical (α_R) region of the Ramachandran map. Phe(6) falls into the bridge region, while Pro(1) adopts a polyproline (P_{II}) conformation (Figure 4, Table 1). Inspection of the hydrogen bond parameters listed in Table S1 (Supporting Information) reveals that both the molecules are stabilized by three intramolecular hydrogen bonds; N(4)···O(1) [N···O = 2.918 Å, H···O = 2.187 Å, ∠N−H···O = 142.7°], N(5)···O(1) [N···O = 2.927 Å, H···O = 2.072 Å, ∠N−H···O = 173°] and N(6)···O(2) [N···O = 2.969 Å, H···O = 2.142 Å, ∠N−H···O = 160.9°] in molecule-A and N(10)···O(7) [N···O = 2.993 Å, H···O = 2.304 Å, ∠N−H···O = 137.2°], N(11)···O(7) [N···O = 3.011 Å, H···O = 2.152 Å, ∠N−H···O = 176.9°] and N(12)···O(8) [N···O = 2.921 Å, H···O = 2.124 Å, ∠N−H···O = 153.8°] in molecule-B. In an ideal continuous 3_{10}-helical conformation, four successive 4→1 hydrogen bonds involving the NH groups of Aib(3), Leu(4), Aib(5), and Phe(6) would have been expected to occur, while an α-helix would yield three successive 5→1 hydrogen bonds. Instead, the amino terminus of the anticipated helix is unfolded, with Pro (1) adopting a semi-extended (P_{II}) conformation. The NH group of residue 3 participates in an intermolecular hydrogen bond.

Packing in crystals may be relevant in evaluating the role of intermolecular interactions in determining the molecular conformation (see Figure S1, Supporting Information). Helical columns of molecules A and B are formed separately and are held together along the b direction by a single intermolecular hydrogen bond N(3)···O(5) ($-x, y+1/2, -z+1$) [N···O = 3.033 Å, H···O = 2.264 Å, ∠N−H···O = 148.9°] of a symmetry related peptide in the case of molecule-A and N(9)···O(11) ($-x-1, y-1/2, -z$) [N···O = 2.998 Å, H···O = 2.180 Å, ∠N−H···O = 158.9°] in the case of molecule-B. Columns of A and B run antiparallel to one another with nonpolar contacts

(21) *Peptides: Synthesis, Structure and Applications*; Gutte, B., Ed.; Academic Press: New York, 1995.
(22) (a) Schneider, T. R.; Sheldrick, G. M. *Acta Crystallogr.* **2002**, *D58*, 1772−1779. (b) Sheldrick, G. M. *SHELXL-97*, A program for the refinement of crystal structures; University of Göttingen: Göttingen, Germany, 1997.
(23) Braunschweiler, L.; Ernst, R. R. *J. Magn. Reson.* **1983**, *53*, 521−528.
(24) (a) Bothner-By, A. A.; Stephens, R. L.; Lee, J.; Warren, C. D.; Jeanloz, R. W. *J. Am. Chem. Soc.* **1984**, *106*, 811−813. (b) Bax, A.; Davis, D. G. *J. Magn. Reson.* **1985**, *63*, 207−213.
(25) Wang, G.; Dunbrack, R. *Bioinformatics* **2003**, *19*, 1589−1591. URL: http://dunbrack.fccc.edu/PISCES.php.
(26) Berman, H.; Westbrook, J.; Feng, Z.; Gilliland, G.; Bhat, T.; Weissig, H.; Shindyalov, I.; Bourne, P. *Nucleic Acids Res.* **2000**, *28*, 235−242.
(27) Gattiker, A.; Gasteiger, E.; Bairoch, A. *Appl. Bioinform.* **2002**, *1*, 107−108. URL: http://us.expasy.org/tools/scanprosite.

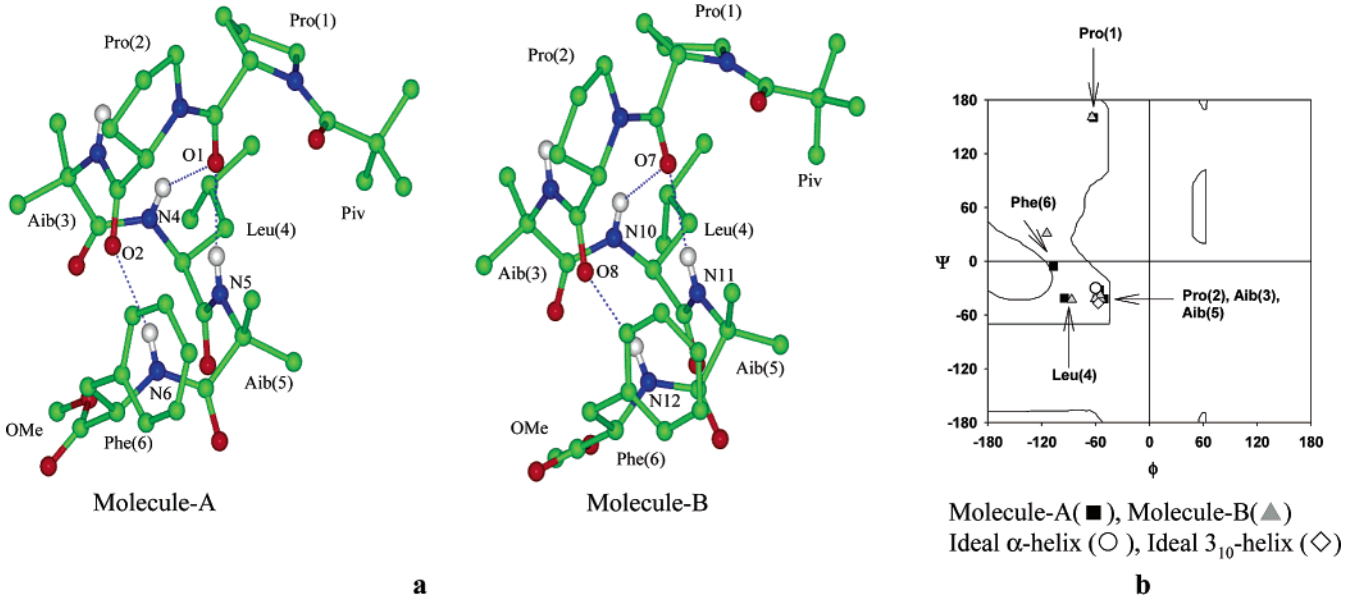

Figure 4. (a) Molecular conformation of peptide **1** (Piv-Pro-Pro-Aib-Leu-Aib-Phe-OMe) in crystals. The two molecules in the asymmetric unit are indicated as Molecule-A and Molecule-B. (b) Ramachandran plot[38] indicating the observed ϕ,ψ values in peptide **1**. Idealized secondary structures are also marked.

Table 1. Torsion Angles (deg)[48] for Peptide 1

	molecule-A			molecule-B		
residues	ϕ	ψ	ω	ϕ	ψ	ω
Pro(1)	−62.4[a]	160.2	−177.7	−63.9[d]	160.7	−178.3
Pro(2)	−50.7	−42.1	−178.2	−53.3	−42.4	−178.5
aib(3)	−55.8	−31.8	179.2	−54.8	−38.1	−177.3
Leu(4)	−94.6	−41.3	−178.5	−86.6	−42.9	−179.5
aib(5)	−58.6	−42.8	−175.2	−60.3	−42.1	−171.7
Phe(6)	−106.7	−5.7[b]	178.6[c]	−114.2	31.0[e]	−176.1[f]
side chains	χ^1		χ^2	χ^1		χ^2
Leu(4)	−64.5		169.6, −68.6	−76.8		172.7, −69.3
Phe(6)	−56.4		−66.2, 109.8	−53.8		−62.3, 117.5

[a] C01′−N1−C1A−C1′. [b] N6−C6A−C6′−O1M. [c] C6A−C6′−O1M−C1M. [d] C02′−N7−C7A−C7′. [e] N12−C12A−C12′−O2M. [f] C12A−C12′−O2M−C2M. Estimated standard deviations are ∼0.5°.

being found along the *c* direction, approximately perpendicular to the helix axis. Figure 5a shows an expanded view of the interactions between the facing molecules A and B, which may be chosen as the crystallographic asymmetric unit. Two nonbonded contacts, which are notable, are between the C$^\alpha$H group in one molecule and the facing Piv carbonyl group on the neighbor (C1A···O02 and C7A···O01). The corresponding parameters for potential C−H···O hydrogen bonds are C1A···O02 = 3.46 Å, H1A···O02 = 2.59 Å, and ∠C1A−H1A···O02 = 149.5°, C7A···O01 = 3.56 Å, H7A···O01 = 2.63 Å, and ∠C7A−H7A···O01 = 160.3°. Figure 5b shows an alternative view of the molecular packing, which illustrates aromatic interactions between the phenylalanine residues of molecule-B in one helical column and a displaced molecule-A in the neighboring helical column. The aromatic rings are approximately parallel (interplanar angle = 14°) with relatively short centroid to centroid distance of 5.25 Å (Figure 5c). The energetic contribution of weak forces like potential C−H···O hydrogen bonds[28] or aromatic interactions[29] are expected to be relatively small (<1 kcal/mol), but may tilt the balance between two possible molecular conformations, when brought into play in a cooperative fashion in crystals.

One question, which remains after examining the crystal structure of peptide **1** is whether crystal packing forces promote unfolding at the N-terminus. To address this issue an NMR analysis of **1** in organic solvents has been carried out.

Solution Conformations of 1. Peptide **1** was examined in three different solvents, chloroform ($CDCl_3$), dimethyl sulfoxide (DMSO-d_6) and methanol (CD_3OH). Spectra were also recorded in a $CDCl_3$ + 10% (v/v) DMSO mixture to enhance NH chemical dispersion to avoid resonance overlap. Resonance assignments of backbone NH and C$^\alpha$H groups were readily achieved using a combination of TOCSY and ROESY/NOESY spectra. Table 2 summarizes NMR parameters for the backbone protons. Figure 6 shows partial NOESY spectra of peptide **1** in $CDCl_3$ illustrating the observed NOEs. Inspection of the region displaying NH ↔ NH connectivity immediately reveals strong successive d_{NN} (NH_i ↔ NH_{i+1} NOEs) characteristic of a helical

(28) (a) Desiraju, G. R.; Steiner, T. *The Weak Hydrogen Bond in Structural Chemistry and Biology*; Oxford University Press: New York, 1999. (b) Gu, Y.; Kar, T.; Scheiner, S. *J. Am. Chem. Soc.* **1999**, *121*, 9411−9422. (c) Vargas, R.; Garza, J.; Dixon, D. A.; Hay, B. P. *J. Am. Chem. Soc.* **2000**, *122*, 4750−4755. (d) Scheiner, S.; Kar, T.; Gu, Y. *J. Biol. Chem.* **2001**, *276*, 9832−9837.

(29) (a) Burley, S. K.; Petsko, G. A. *Science* **1985**, *229*, 23−28. (b) Sun, S.; Bernstein, E. R. *J. Phys. Chem.* **1996**, *100*, 13348−13366. (c) Hunter, C. A.; Lawson, K. R.; Perkins, J.; Urch, C. J. *J. Chem. Soc., Perkin Trans. 2* **2001**, 651−669. (d) Chelli, R.; Gervasio, F. L.; Procacci, P.; Schettino, V. *J. Am. Chem. Soc.* **2002**, *124*, 6133−6143. (e) Tatko, C. D.; Waters, M. L. *J. Am. Chem. Soc.* **2002**, *124*, 9372−9373. (f) Aravinda, S.; Shamala, N.; Das, C.; Sriranjini, A.; Karle, I. L.; Balaram, P. *J. Am. Chem. Soc.* **2003**, *125*, 5308−5315.

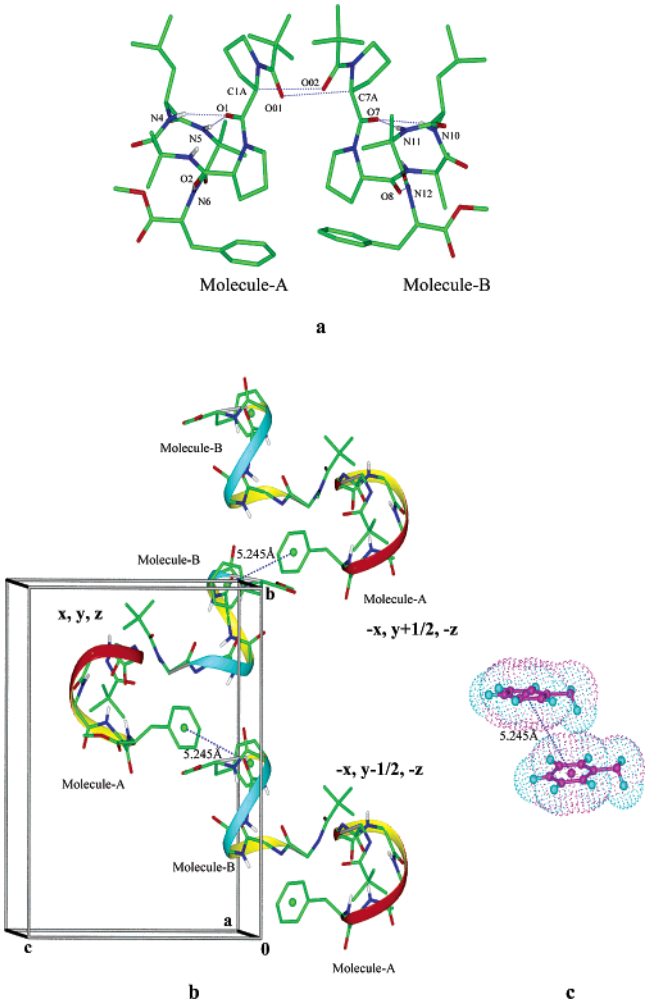

Figure 5. (a) Asymmetric unit of peptide **1** (Piv-Pro-Pro-Aib-Leu-Aib-Phe-OMe). The potential C−H···O hydrogen bonds are shown as dotted lines. The figure was generated using the program MOLMOL.[51] (b) The aromatic interaction observed in peptide **1**. (c) A view of the geometry of Phe-Phe interactions.

conformation over the segment residues 3 to 6 (bottom panel). Two critical NOEs which establish the possible conformations of the Pro-Pro segment are also observed (top panel); the Pro(1)$C^{\alpha}H$ ↔ Pro(2)$C^{\delta}H_2$ ($d_{\alpha\delta}^{1,2}$) and the Pro(1)$C^{\delta}H_2$ ↔ Pro(2)-$C^{\delta}H_2$ ($d_{\delta\delta}^{1,2}$) NOEs. The simultaneous observation of these two NOEs clearly suggests the population of at least two distinct conformational species, corresponding to the P_{II} and α_R conformations at Pro(1). The relevant inter proton distances in the two possible conformations of the diproline segment are: α_R-$\alpha_R \leq 3.3$Å ($d_{\delta\delta}^{1,2}$) and P_{II}-$\alpha_R \approx 2.2$Å ($d_{\alpha\delta}^{1,2}$). In addition, a minor conformation in slow exchange on the NMR time scale is characterized as the Pro(1)-Pro(2) *cis* form by the observation of the Pro(1)$C^{\alpha}H$ ↔ Pro(2) $C^{\alpha}H$ NOE. Figure 7 illustrates additional NOEs characteristic of the continuous helical conformation spanning residues 1 to 5 of peptide **1**. These are the Pro(1)$C^{\alpha}H$ ↔ Leu(4)NH, Pro(2)$C^{\alpha}H$ ↔ Leu(4)NH and Leu-(4)$C^{\alpha}H$ ↔ Phe(6)NH. In an α-helical conformation the d_{NN} and $d_{\alpha N}(i,i+3)$ inter-proton distances are < 3.5 Å. In addition, in a 3_{10}-helical segment $d_{\alpha N}(i,i+2)$ NOEs may also be observed as the estimated distance ≈3.8 Å. Interestingly, a $d_{\alpha N}(i,i+4)$ NOE is also observed in Figure 7, (Pro(2)$C^{\alpha}H$ ↔ Phe(6)NH). In an α-helix this distance would be ∼4.2 Å.[30] The NOE evidence is thus strongly suggestive of a significant population of a continuous helix over residues 1 to 5, encompassing the amino terminus diproline segment. Studies in $CDCl_3$+10% DMSO were also supportive of a helical conformation over residues 2 to 5 (Supporting Information), but definitive evidence for a population of the α_R conformation at Pro(1) could not be obtained due to resonance overlap of $C^{\delta}H_2$ protons. In the minor *cis* Pro-Pro conformer, observed NOEs Pro(2)$C^{\delta}H_2$ ↔ Aib(3)-NH and Pro(2)$C^{\alpha}H$ ↔ Aib(5)NH are also supportive of a helical conformation over the 2−5 segment. This is more elaborately discussed in considering the results for peptide **2**. Further, the NOEs, Pro(1)$C^{\alpha}H$ ↔ Aib(3)NH and Pro(1)$C^{\alpha}H$ ↔ Aib(4)NH are confirmatory of a *cis* Pro(1)-Pro(2) geometry.

To delineate the number of intramolecular hydrogen bonded NH groups a solvent titration experiment was carried out, by adding the strongly hydrogen bonding solvent DMSO to the apolar solvent, $CDCl_3$. Figure 8 establishes that Aib(3) NH displays a high degree of solvent sensitivity moving rapidly downfield upon addition of DMSO. This behavior contrasts with much smaller effects observed on the NH groups of Leu(4), Aib(5), and Phe(6), supporting their involvement in intramolecular hydrogen bonding. The solvent dependence of the Aib-(3)NH resonance, even at very low DMSO concentrations is *monotonic*, ruling out the possibility of a solvent induced conformational transition, occurring sharply over a narrow range of DMSO concentration. The observed solvent dependence is, however, consistent with an equilibrium mixture of conformers in $CDCl_3$ in which the Aib(3) NH is hydrogen bonded in one conformer and solvent exposed in the other. Specific solvation by the cosolvent DMSO is expected to shift the equilibrium in favor of a non-hydrogen bonded structure at higher DMSO concentration. The temperature dependence of NH chemical shifts in DMSO and CD_3OH was also examined and the temperature coefficients listed in Table 2 and Supporting Information. It is again evident that the Aib(3) NH group is solvent exposed, showing a large temperature coefficient in both the solvents, whereas the remaining three NH groups have significantly smaller temperature dependences. The presence of a signification fraction of helical conformers, in which the Pro-(1)-Pro(2) type I/III β-turn is formed with consequent involvement of Aib(3)NH in an intramolecular hydrogen bond is supported by the NOEs discussed earlier. The NMR data thus suggest that although Aib(3) NH appears solvent exposed, there is clear evidence for a substantial population of helical conformations encompassing the diproline segment, in an apolar medium like $CDCl_3$. The predominant species in more polar media lack a 4→1 hydrogen bond between the Piv CO and Aib-(3) NH group, thus arguing against a Pro(1)-Pro(2) type I/III β-turn.

Evidence for dynamic exchange between distinct conformational species is also obtained from the temperature dependence of ^{1}H NMR spectra in $CDCl_3$. Inspection of the backbone $C^{\alpha}H$ and NH resonances over the temperature range 275 to 323K reveals selective broadening of specific resonances. Figure 9 illustrates selective line broadening observed in Pro(1) $C^{\alpha}H$, Leu(4) $C^{\alpha}H$, Leu(4) NH, and Aib(3) NH resonances. Exchange broadening is most dramatically manifested when the rate constant (k, s^{-1}) for interconversion is approximately the same as the frequency difference for the observed nucleus in the two

(30) Wüthrich, K. *NMR of Proteins and Nucleic Acids*; John Wiley & Sons: New York, 1986.

Table 2. NMR Parameters for the Peptides **1** and **2**

residue		peptide 1					peptide 2				
		$CDCl_3$		CD_3OH[a]			$CDCl_3$ + 4.25% DMSO-d_6			CD_3OH[a]	
		chemical shift (ppm)		chemical shift (ppm)		dδ/dT (ppb/K)	chemical shift (ppm)		dδ/dT (ppb/K)	chemical shift (ppm)		dδ/dT (ppb/K)
1	**2**	NH	$C^{\alpha}H$	NH	$C^{\alpha}H$		NH	$C^{\alpha}H$		NH	$C^{\alpha}H$	
	Aib 1						5.35		−6.34	7.36	−	−8.52
							5.39*		−3.53*			
Pro 1/	Pro 2		4.48		4.64			4.56			4.68	
			4.45*					4.50*				
Pro 2/	Pro 3		4.28		4.29			4.35			4.30	
			4.31*					4.31*				
Aib3/	Aib 4	6.92		8.15		−7.24	7.50		−3.41	8.21	−	−7.78
		7.55*					7.93*		−2.51*			
Leu 4/	Val5	7.55	4.11	7.89	3.93	−3.02	7.65	4.21	−2.42	7.47	4.09	−3.58
		6.89*	4.29*				6.74*	4.10*	−1.98*			
Aib 5/	Ala 6	7.26		7.73		−1.32	7.57	4.41	−3.56	8.03	4.24	−6.59
		6.87*					7.59*	4.48*	−4.78*			
Phe 6/	Phe 7	7.44	4.76	7.72	4.60	−4.57	7.46	4.74	−4.81	8.13	4.62	−5.08
		7.12*	4.77*				7.54*	4.75*	−5.76*			

[a] In CD_3OH, minor resonances are overlapped more closely with resonances of the major species. *Corresponds to the minor Pro-Pro *cis* conformation.

distinct conformations (ν_A-ν_B, Hz). Exchange effects in peptide **1** are also observed in temperature dependent ^{13}C spectra, with the Pro(1) C^{α} carbon being dramatically broadening at 275 K as compared to the Pro(2) C^{α} carbon (Figure 9). Line broadening effects observed in both ^1H and ^{13}C spectra suggest that the conformational process involves the N-terminus residues in the peptide, consistent with the suggestion that dynamic exchange is observed between the α_R-α_R and P_{II}-α_R conformations of the diproline segments.

The NMR results are thus largely consistent with a solvent dependent conformational equilibrium; a continuous helical conformation predominating in poorly solvating media. Solvent competition for hydrogen bonds tilts the balance in favor of the P_{II}-α_R conformation observed in crystals, suggesting that packing effects may not be a major determinant.

Solution Conformation of 2. The finding that the Pro(1) conformation in peptide **1** is solvent dependent led us to investigate peptide **2** in which an additional Aib residue was placed at the N-terminus of the Pro-Pro segment. Our hope was that intramolecular hydrogen bond formation involving the Aib-(4) NH group with either Aib(1) CO (4→1) or with Boc CO (5→1) would lead to a stable helix nucleating turn. Both these conformations would require that Pro(1) adopts a helical (α_R) conformation. Peptide **2** was readily soluble in organic solvents and the NMR studies were carried out in $CDCl_3$+4.25% DMSO-d_6 (v/v) and methanol. Additional resonances are observed, corresponding to an appreciable population of the *cis* conformation (∼20%) about the Pro(2)−Pro(3) bond. The assignment of the minor conformer to the *cis* Pro-Pro geometry is confirmed by the observation of strong NOEs between Pro(2) $C^{\alpha}H$ and Pro(3) $C^{\alpha}H$ of the minor species. Assignment of the major species to the *trans* form is confirmed by the observation of strong NOEs between Pro(2)$C^{\alpha}H$ and Pro(3)$C^{\delta}H_2$ protons (Figure 10). NMR parameters are listed in Table 2. The succession of NH_i ↔ NH_{i+1} NOEs (d_{NN} NOEs) observed for the segment 4 to 7 strongly supports a significant population of helical conformations at the C-terminus.

The strong NOEs observed between Aib(1) NH and Pro(2) $C^{\delta}H_2$ protons in both *trans* and *cis* conformers suggests that Aib(1) adopts a local helical conformation in both cases. In the major conformation, the Pro(2)$C^{\alpha}H$ ↔ Pro(3)$C^{\delta}H_2$ NOE is strong suggesting a significant population of the P_{II} conformation at this residue ($\psi \approx 120°$). The Pro(2)$C^{\delta}H_2$ ↔ Pro(3)$C^{\delta}H_2$ NOE, which would constitute the signature of a local α_R conformation at Pro(2) is not readily detectable because of resonance overlap. Aib(4) NH exhibits NOEs to the preceding Pro(3)$C^{\delta}H$ residue and the NH of succeeding Val(5) residue in both *cis* and *trans* conformations, supporting a local helical conformation for the 3 to 5 segment. The temperature coefficients of NH chemical shifts measured in $CDCl_3$ + 4.25% DMSO-d_6 (v/v) reveal that Aib (1) NH, which has a large $d\delta$/dT value, is solvent exposed. Interestingly, Aib (4) NH has much lower temperature coefficient than the corresponding residue in peptide **1** (Aib(3) NH, Table 2). In the *cis* isomer, extremely low dδ/dT values are observed for both Aib(4) and Val(5) NH groups, suggestive of their involvement in intramolecular hydrogen bonds. In CD_3OH, the observed dδ/dT values for both conformers are appreciably larger, indicative of a much smaller population of folded intramolecular hydrogen bonded conformations, presumably as a result of solvent competition for donor and acceptor sites.

The critical issue in the analysis of peptide **2** is whether the Aib-Pro-Pro-Aib segment forms a helical turn (α_R-α_R-α_R-α_R) in an all *trans* conformation. There is also the additional issue of the precise conformation of the segment in the *cis* form. The NMR evidence presented above supports the involvement of Aib(4) NH in intramolecular hydrogen bond formation in both *trans* and *cis* forms. In the *trans* conformer the observed pattern of NOEs is consistent with the formation of a helical turn which may involve a 5→1 hydrogen bond between the Boc CO and the Aib(4) NH, although the alternative 4→1 hydrogen bond between Aib(1) CO and Aib(4) NH cannot be ruled out. Such bifurcated interactions are relatively common in peptides and proteins.[31] The NOE evidence also supports the coexistence of a fraction of molecules with Pro(2)in the P_{II} conformation. A continuous helical conformation consistent with the NMR data, has been obtained by placing all residues in the ideal α_R ($\phi \approx -60°$, $\psi \approx -30°$) conformation followed by minimization. No

(31) (a) Baker, E. N.; Hubbard, R. E. *Prog. Biophys. Mol. Biol.* **1984**, *44*, 97−179. (b) Datta, S.; Shamala, N.; Banerjee, A.; Balaram, P. *J. Pept. Res.* **1997**, *49*, 604−611. (c) Steiner, T. *Angew. Chem., Int. Ed.* **2002**, *41*, 48−76.

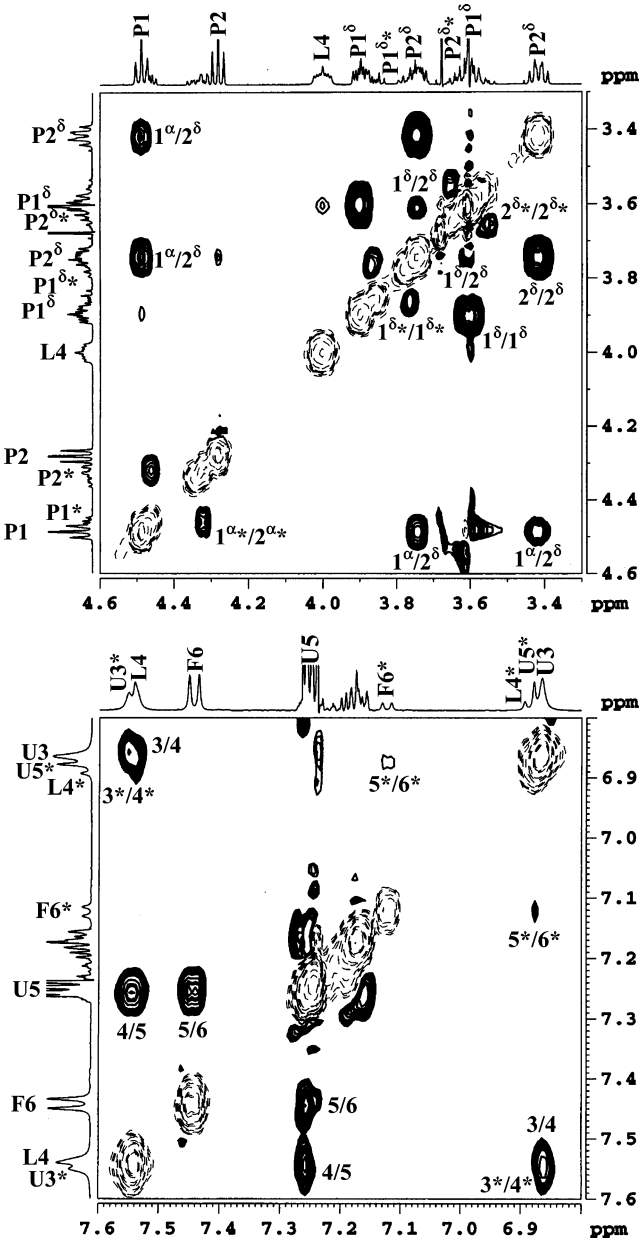

Figure 6. Partial 500 MHz NOESY spectra of peptide **1** in $CDCl_3$ at 300 K. (Top panel) Pro(1)$C^{\alpha}H$ ↔ Pro(2)$C^{\delta}H$ and Pro(1)$C^{\delta}H$ ↔ Pro(2)$C^{\delta}H$ NOEs and (bottom panel) NH ↔ NH NOEs. (U, Aib). * Corresponds to the minor conformation.

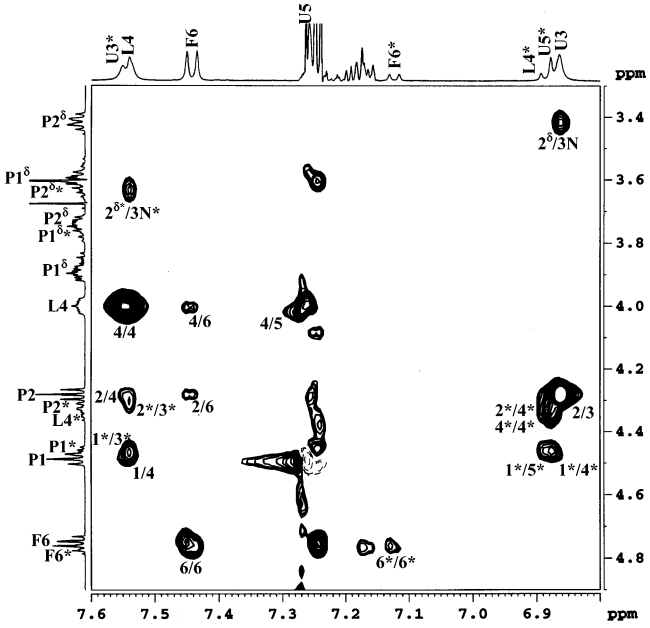

Figure 7. Partial 500 MHz NOESY spectrum of peptide **1** highlighting $C^{\alpha}H$ ↔ NH NOEs in $CDCl_3$ at 300 K. * Corresponds to the minor conformation.

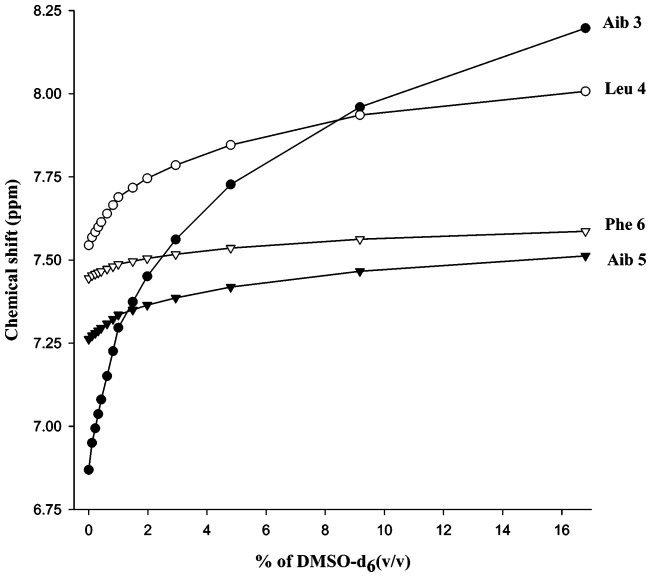

Figure 8. Solvent dependence of NH chemical shifts in peptide **1**, at varying concentrations of DMSO-d_6 in $CDCl_3$.

sterically unfavorable contacts are observed in this model (Figure S2a, Supporting Information). Clearly, peptide **2** appears to be a more promising candidate in our attempts to design a diproline nucleated helical turn. The NMR data for the *cis* form supports the type VI β-turn conformation,[2b,3c,7b,32] with the Pro-Pro segment occupying the $i+1$ and $i+2$ positions, stabilized by a 4→1 hydrogen bond between the Aib(1)CO and Aib(4) NH groups. The ideal torsion angles for the type VIa β-turn are Pro(2) ($\phi \approx -60°$, $\psi \approx 120°$) Pro(3)($\phi \approx -90°$, $\psi \approx 0°$). This places Pro(3) in the right-handed helical region (α_R) of conformational space, permitting nucleation of a helix beyond residues 3. An acceptable model was generated by using idealized type VIa β-turn backbone torsion angles and ideal α_R values for residues 4 to 7 followed by a few cycles of minimization to relieve short contacts (Figure S2b, Supporting Information). An α_R conformation at Aib(4) results in a 5→1 hydrogen bond between Val(5) NH and Aib(1) CO groups. The conformational features observed in the *cis* form can formally be designated as an α-turn. Interestingly, the characterization of isolated α-turns in proteins[33] has revealed a family with a *cis* peptide bond between residues i+1 and i+2.[33b] The results on peptide **2** are, thus, largely similar to those obtained for peptide **1**, suggesting that N-terminus extension with an obliga-

(32) (a) Richardson, J. S. *Adv. Protein Chem.* **1981**, *34*, 167−339. (b) Wilmot, C. M.; Thornton, J. M. *Protein Eng.* **1990**, *3*, 479−493. (c) Muller, G.; Gurrath, M.; Kurz, M.; Kessler, H. *Proteins* **1993**, *15*, 235−251. (d) Yao, J.; Fehrer, V. A.; Espejo, B. F.; Reymond, M. T.; Wright, P. E.; Dyson, H. J. *J. Mol. Biol.* **1994**, *243*, 736−753. (e) Yao, J.; Bruschweiler, R.; Dyson, H. J.; Wright, P. E. *J. Am. Chem. Soc.* **1994**, *116*, 12051−12052. (f) Halab, L.; Lubell, W. D. *J. Am. Chem. Soc.* **2002**, *124*, 2474−2484. (g) Guruprasad, K.; Rajkumar, S. *J. Biosciences* **2000**, *25*, 143−156. (h) Meng, H. Y.; Thomas, K. M.; Lee, A. E.; Zondlo, N. J. *Biopolymers (Peptide Science)* **2006**, *84*, 192−204.

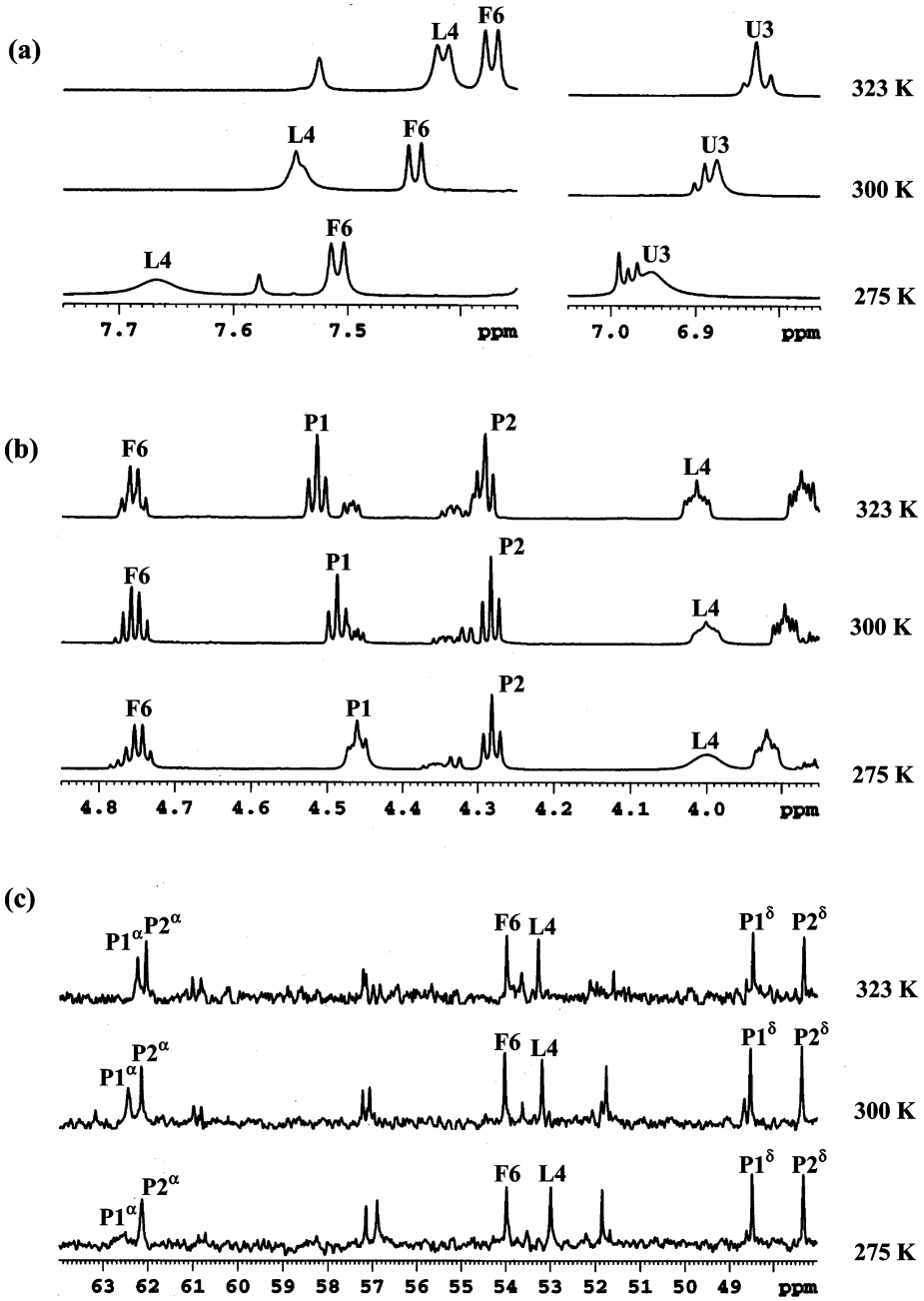

Figure 9. Partial ^{1}H and ^{13}C NMR spectra of peptide **1** in $CDCl_3$ at different temperatures illustrating selective line broadening of (a) Aib(3) and Leu(4) amide protons (b) Pro(1) $C^{\alpha}H$ and Leu (4) $C^{\alpha}H$ resonances and (c) Pro(1) C^{α} carbon resonance.

tory helical residue has not significantly altered the conformational distribution at the diproline segment.

Analysis of Diproline Segments in Proteins. Before discussing the implication of the results obtained on peptides **1** and **2**, it is useful to examine the conformational properties of diproline segments in proteins. Using a data set of 1741 protein chains obtained from crystal structures a total of 462 Pro-Pro units were obtained. The results are summarized in Table 3. It is clear that the overwhelming majority of examples correspond to the *trans*−*trans* family. The *cis-trans* form and the *trans-cis* loops are almost equally populated, while only one example of a *cis-cis* structure was observed. The conformational distribution in the *trans-trans* family reveals that the P_{II}-P_{II} (polyproline structure) is observed in 229 (56%) cases. Notably the polyproline structure is now being suggested as a major component of segments of globular protein chains, which were hitherto considered as unstructured.[34] The P_{II} conformation appears to be highly favored even for nonproline residues.[35] The P_{II}-α conformation for the diproline segment is also significantly

(33) (a) Pavone, V.; Gaeta, G.; Lombardi, A.; Nastri, F.; Maglio, O.; Isernia, C.; Saviano, M. *Biopolymers* **1996**, *38*, 705−721. (b) Nataraj, D. V.; Srinivasan, N.; Sowdhamini, R.; Ramakrishnan, C. *Curr. Sci.* **1995**, *69*, 434−447. (c) Dasgupta, B.; Pal, L.; Basu, G.; Chakrabarti, P. *Proteins: Struct. Funct. Bioinformatics* **2004**, *55*, 305−315.

(34) (a) Shi, Z.; Woody, R. W.; Kallenbach, N. R. *Adv. Protein Chem.* **2002**, *62*, 163−240. (b) Cao, W.; Bracken, W. C.; Kallenbach, N. R.; Lu, M. *Protein Sci.* **2004**, *13*, 177−189. (c) Rath, A.; Davidson, A. R.; Deber, C. M. *Biopolymers (Peptide Science)* **2005**, *80*, 179−185. (d) Shi, Z.; Chen, K.; Liu, Z.; Ng, A.; Bracken, W. C.; Kallenbach, N. R. *Proc. Natl. Acad. Sci. U.S.A.* **2005**, *102*, 17964−17968.

(35) (a) Chellgren, B. W.; Creamer, T. P. *Biochemistry* **2004**, *43*, 5864−5869. (b) Kentsis, A.; Mezei, M.; Osman, R. P. *Proteins: Struct. Funct. Bioinformatics* **2005**, *61*, 769−776.

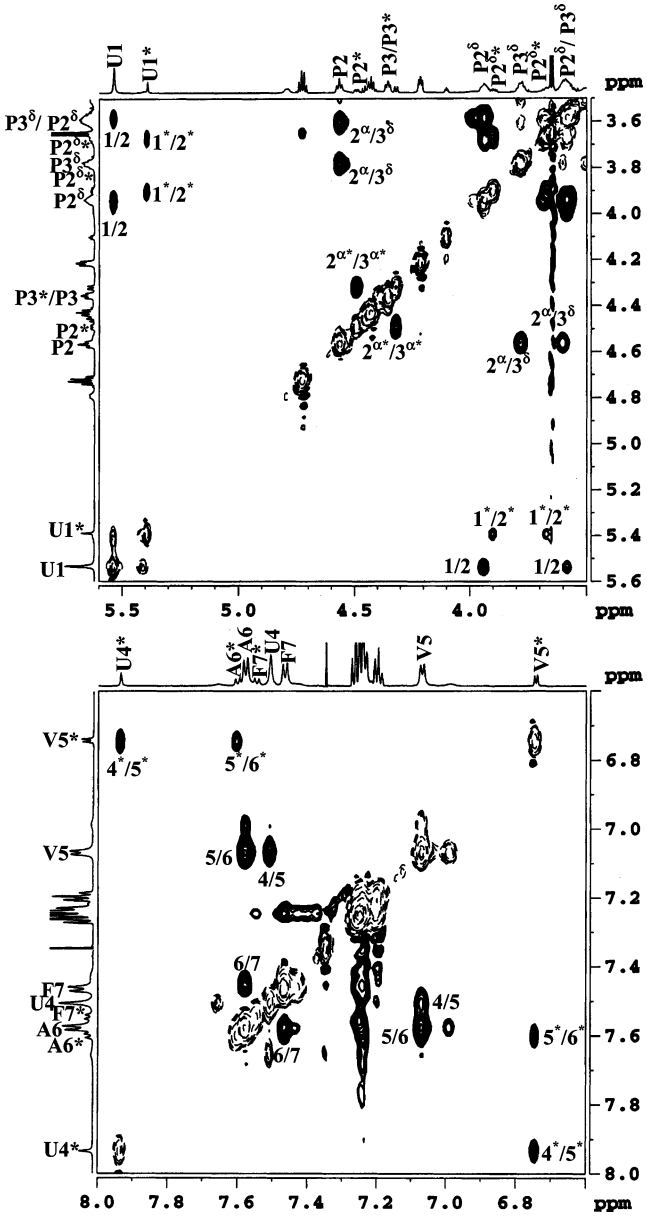

Figure 10. Partial 500 MHz ROESY spectra of peptide **2** in $CDCl_3$ + 4.25% DMSO-d_6 highlighting NOEs in $C^{\alpha}H \leftrightarrow C^{\alpha}H$ (top) and NH ↔ NH (bottom) regions. * Corresponds to the minor conformation.

Table 3. Conformation of Pro-Pro Segments in Proteins

type	*cis-cis*	*cis-trans*	*trans-cis*	*trans-trans*
α-α	−	−	−	25
α-P_{II}	−	−	−	−
P_{II}-α	−	5	−	129
P_{II}-P_{II}	1	17	9	229
P_{II}-bridge	−	1	19	19
others	−	1	−	7
total	1	24	28	409
%	0.22	5.19	6.06	88.53

populated, with 129 (31.5%) falling into this category. Interestingly, no case of an α-P_{II} structure was identified. The helical diproline segment (α_R-α_R), which is of special interest to the present study was observed in 25 examples. These were further subdivided into long helices (residue length ≥7 residues) in 15 examples and short helices (residue length ≤ 6) in 10 examples. In the long helices, 10 contained the diproline segment at the amino terminus, with 4 examples of centrally positioned Pro-Pro segments and 1 example at the C-terminus. In all cases of short helices, the Pro-Pro residues are at the N-terminus. These observations suggest that the α_R-α_R conformation is indeed accessible for diproline segments and may be stabilized under specific conditions. The objective of a synthetic design strategy must therefore be to optimize factors which promote the α_R-α_R conformations in diproline segments.

Energetics of Alternate Diproline Conformations. The purpose of the present study was to establish conditions under which the diproline unit could be induced to adopt a stable helical conformation. In peptides **1** and **2**, the population of *cis* conformations about the X-Pro bond was eliminated by using bulky preceding residues/blocking groups, leaving *cis-trans* isomerization about the Pro-Pro bond as the only conformational possibility. The additional degrees of freedom, Pro(1) ψ and Pro(2) ψ, remain to be considered; assuming only two broad conformational possibilities α_R and P_{II} (note that the C_7, γ turn conformation $\phi \approx -70°$, $\psi \approx +70°$ is not considered as a separate structure, but included along with P_{II} in the nonhelical set).

Peptide **1** in crystals revealed a P_{II}-α_R structure. Interestingly, even in the poorly solvating medium $CDCl_3$ the P_{II}-α_R conformation appears to be significantly populated suggesting that the potential formation of an additional intramolecular 4→1 hydrogen bond between the Piv(CO) and Aib(3) NH groups in an α_R-α_R structure does not override other factors contributing to the favorable free energy of the P_{II}-α_R conformation. To examine whether there are specific unfavorable interactions *destabilizing* the α_R-α_R structure, energy calculations (in vacuo) were carried out on a structure based on the conformation in crystals and a model continuous helix generated by placing Pro-(1) in the α_R region. Minimization of the energy of the crystal conformer converged to a structure almost identical to that observed in the solid-state structure (Figure 11). Surprisingly, both optimized models have very similar energies revealing no obviously unfavorable interatomic interactions. Figure 11 summarizes schematically the results of the conformational analysis of peptide **1** in solution. Three distinct species are detectable. The Pro(1)−Pro(2) *cis* form is minor conformer (26%), which is in slow exchange with the major *trans* conformations on the NMR time scale, because of the significant kinetic barrier to interconversion. The two *trans* forms (α_R-α_R and P_{II}-α_R at the diproline segment) are in rapid, dynamic equilibrium on the NMR time scale, resulting in averaged chemical shifts. NOEs however provide an important diagnostic for the simultaneous presence of both conformers. Interconversion between the two states requires only a change of Pro(1) ψ from the P_{II} to α_R region of ϕ,ψ space. Such transitions have been estimated to have activation barriers of ∼14 kcal mol^{-1}.[36]

Discussion

The conformation of proline containing peptides and polypeptides has been the subject of intense investigation for half a century. The Ramachandran−Kartha model for collagen and subsequent work on polyproline and collagen models clearly established the unique influences of this residue on polypeptide stereochemistry.[37,38] Three features of the proline residue are

(36) (a) Nagaraj, R.; Venkatachalapathi, Y. V.; Balaram, P. *Int. J. Peptide Protein Res.* **1980**, *16*, 291−298. (b) Deber, C. M.; Fossel, E. T.; Blout, E. R. *J. Am. Chem. Soc.* **1974**, *96*, 4015−4017.

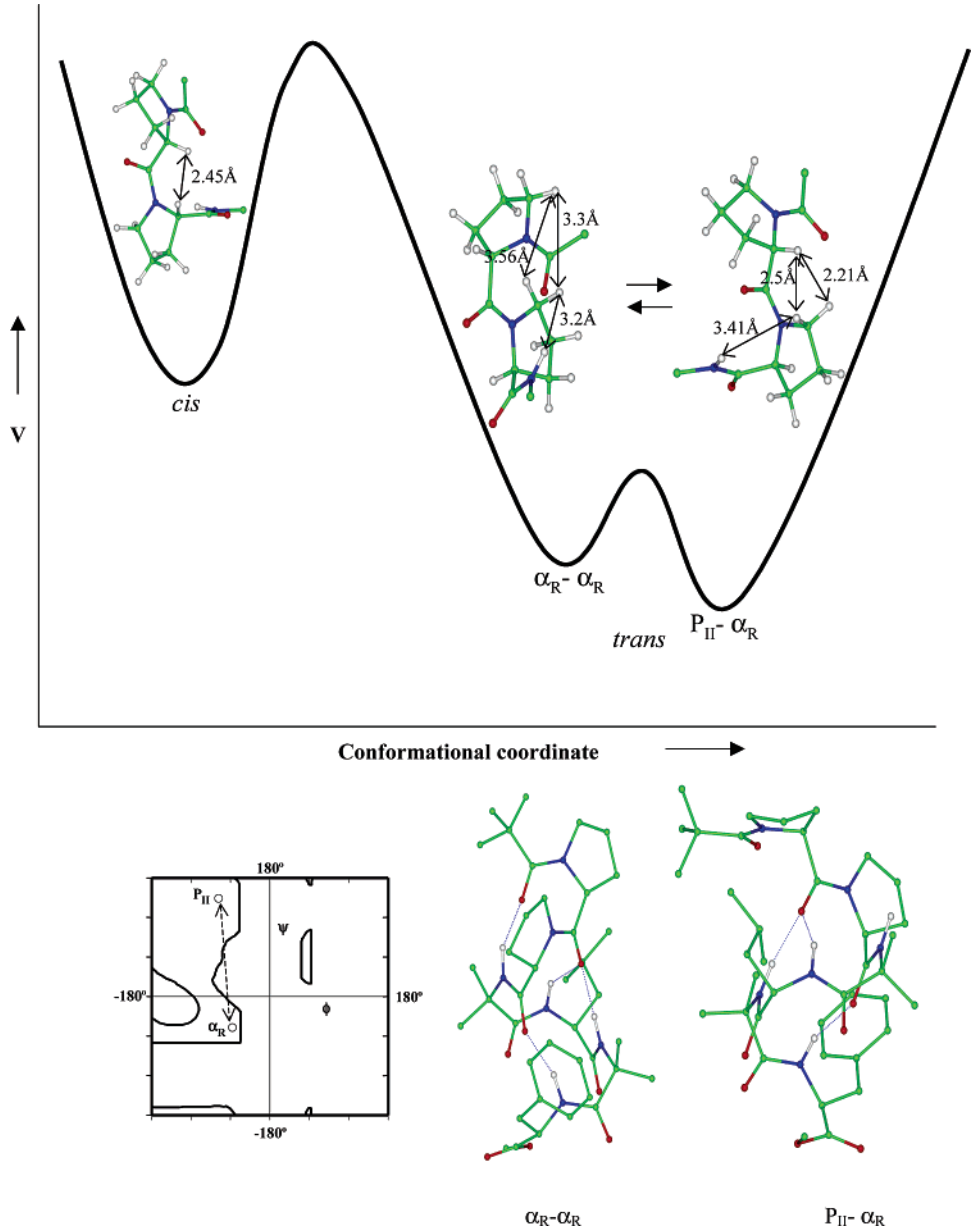

Figure 11. Schematic representation of conformational distribution for **1** in solution (top). The Ramachandran map showing the possible two conformations for proline (P_{II} and α_R) and the energy minimized model of peptide **1** in the *trans* form (α_R-α_R and P_{II}-α_R) (bottom).

specifically important: (i) The ability of the X−Pro bond to adopt the *cis* conformation, with the energetic differences between the *cis* and *trans* forms being influenced by the preceding residue.[19,39] (ii) The puckering of the five membered pyrolidine ring, which influences backbone conformational choice resulting in a complex inter-relationship between ring geometry and local structure.[40] (iii) The interplay between the polyproline P_{II} and α_R conformations at the Pro residue, which determines the turn type and local nucleating structures.[41] A

(37) (a) Ramachandran, G. N.; Kartha, G. *Nature (London)* **1954**, *174*, 269−270. (b) Ramachandran, G. N.; Kartha, G. *Nature (London)* **1955**, *176*, 593−595. (c) Rich, A.; Crick, F. H. C. *Nature (London)* **1955**, *176*, 915−916. (d) Rich, A.; Crick, F. H. C. *J. Mol. Biol.* **1961**, *3*, 483−506. (e) Ramachandran, G. N. *Int. J. Peptide Protein Res.* **1988**, *31*, 1−16. (f) Bella, J.; Eaton, M.; Brodsky, B.; Berman, H. M. *Science* **1994**, *266*, 75−81. (g) Kramer, R. Z.; Vitagliano, L.; Bella, J.; Berisio, R.; Mazzarella, L.; Brodsky, B.; Zagari, A.; Berman, H. M. *J. Mol. Biol.* **1998**, *280*, 623−638. (h) Kramer, R. Z.; Bella, J.; Brodsky, B.; Berman, H. M. *J. Mol. Biol.* **2001**, *311*, 131−147. (i) Creamer, T. P.; Campbell, M. N. *Adv. Protein Chem.* **2002**, *62*, 263−282. (j) Vila, J. A.; Baldoni, H. A.; Ripoll, D. R.; Ghosh, A.; Scheraga, H. A. *Biophys. J.* **2004**, *86*, 731−742. (k) Brodsky, B.; Persikov, A. V. *Adv. Protein Chem.* **2005**, *70*, 301−339.
(38) Ramachandran, G. N.; Sasisekharan, V. *Adv. Protein Chem.* **1968**, *23*, 284−438.
(39) (a) MacArthur, M. W.; Thornton, J. M. *J. Mol. Biol.* **1991**, *218*, 397−412. (b) Reimer, U.; Scherer, G.; Drewello, M.; Kruber, S.; Schutkowski, M.; Fischer, G. *J. Mol. Biol.* **1998**, *279*, 449−460. (c) Pal, D.; Chakrabarti, P. *J. Mol. Biol.* **1999**, *294*, 271−288. (d) Bhattacharyya, R.; Chakrabarti, P. *J. Mol. Biol.* **2003**, *331*, 925−940. (e) Pahlke, D.; Freund, C.; Leitner, D.; Labudde, D. *BMC Struct. Biol.* **2005**, *5*, 8.
(40) (a) Milner-White, E. J.; Bell, L. H.; Maccallum, P. H. *J. Mol. Biol.* **1992**, *228*, 725−734. (b) Chakrabarti, P.; Pal, D. *Prog. Biophys. Mol. Biol.* **2001**, *76*, 1−102. (c) Vitagliano, L.; Berisio, R.; Mastrangelo, A.; Mazzarella, L.; Zagari, A. *Protein Sci.* **2001**, *10*, 2627−2632. (d) Ho, B. K.; Coutsias, E. A.; Seok, C.; Dill, K. A. *Protein Sci.* **2005**, *14*, 1011−1018. (e) Eberhardt, E. S.; Loh, S. N.; Hinck, A. P.; Raines, R. T. *J. Am. Chem. Soc.* **1992**, *114*, 5437−5439. (f) Panasik, N., Jr.; Eberhardt, E. S.; Edison, A. S.; Powell, D. R.; Raines, R. T. *Int. J. Peptide Protein Res.* **1994**, *44*, 262−269. (g) Eberhardt, E. S.; Panasik, N., Jr.; Raines, R. T. *J. Am. Chem. Soc.* **1996**, *118*, 12261−12266. (h) DeRider, M. L.; Wilkens, S. J.; Waddell, M. J.; Bretscher, L. E.; Weinhold, F.; Raines, R. T.; Markley, J. L. *J. Am. Chem. Soc.* **2002**, *124*, 2497−2505.
(41) (a) Kang, Y. K. *J. Phys. Chem.* **1996**, *100*, 11589−11595. (b) Kang, Y. K.; Jhon, J. S. *J. Peptide Res.* **1999**, *53*, 30−40. (c) Kang, Y. K.; Choi, H. Y. *J. Biophy. Chem.* **2004**, *111*, 135−142. (d) Némethy, G.; Gibson, K. D.; Palmer, K. A.; Yoon, C. N.; Paterlini, G.; Zagari, A.; Rumsey, S.; Scheraga, H. A. *J. Phys. Chem.* **1992**, *96*, 6472−6484.

resurgence of interest in the P_{II} conformation as a favored state for non-Pro residues has also followed the recognition that "unstructured" polypeptide chains may be relevant in determining the biological function of specific classes of proteins.[34] The present study was conceived with the simple goal of asking if an N-terminal diproline segment could adopt an α_R-α_R conformation, thereby facilitating helix nucleation. Structural studies of the model peptide **1** (Piv-Pro-Pro-Aib-Leu-Aib-Phe-OMe) establish that in solution both α_R-α_R and P_{II}-α_R conformations are present in inert solvents, while the later predominate in strongly solvating media. Inspection of models and energy minimization studies do not reveal any obvious unfavorable interaction, which destabilize the α_R conformation of Pro(1) with respect to the P_{II} structure. It is possible that entropic factors favor the P_{II} conformation, in solution, offsetting any enthalpic gain, which may be achieved by the formation of an additional hydrogen bond in a continuous helix. The observation of the P_{II}-α_R structure in a relatively inert solvent provides support for this line of reasoning. In crystals, the intermolecular N(3)···O(5)/N(9)···O(11) hydrogen bond (Table S1, Supporting Information) provides a stabilizing interaction compensating for the absence of an intramolecular hydrogen bond. Crystal state conformations are sometimes considered to result from the imperative to maximize intermolecular packing interactions. This does not seems to the case in peptide **1**, where the conformations determined in the crystal are also significantly populated in solution. The growing body of literature on the P_{II} conformation of nonproline residues raises several issues that need to be addressed on the origins of the stability of this structure.[34a,37e,42] While hydration effects have been advanced as a possible cause in collagen models,[43] stereoelectronic considerations also merit attention.[44] In the present study the P_{II} conformation at Pro(1) clearly does not result from backbone solvation effects since it is also observed in inert solvents like chloroform.

Is there a relationship between the observed puckering of the proline ring[40] and the backbone conformation? Figure 12 shows a view of the proline rings in the crystal structure of **1** and an example of the helical diproline (α_R-α_R) segment in a protein structure.[9] In **1** the Pro-Pro segment adopts a C$^\gamma$-*endo*−C$^\gamma$-*exo* conformation, whereas in the protein example the observation is C$^\gamma$-*exo*−C$^\gamma$-*exo* (exo/UP: negative χ^1 and χ^3, positive χ^2 and χ^4; endo/DOWN: Positive χ^1 and χ^3, negative χ^2 and χ^4).[40,45] Examination of all the 25 diproline segments in the α_R-α_R conformation observed in proteins, revealed 18 examples of C$^\gamma$-*exo*−C$^\gamma$-*exo*, 6 examples of C$^\gamma$-*exo*−C$^\gamma$-*endo* and one example of C$^\gamma$-*endo*−C$^\gamma$-*endo* conformations. Interestingly, no example of the C$^\gamma$-*endo*−C$^\gamma$-*exo* conformation was observed in the helical diproline segments. The influence of the preceding residue on the conformation of the Pro(1) pyrolidine ring and consequently

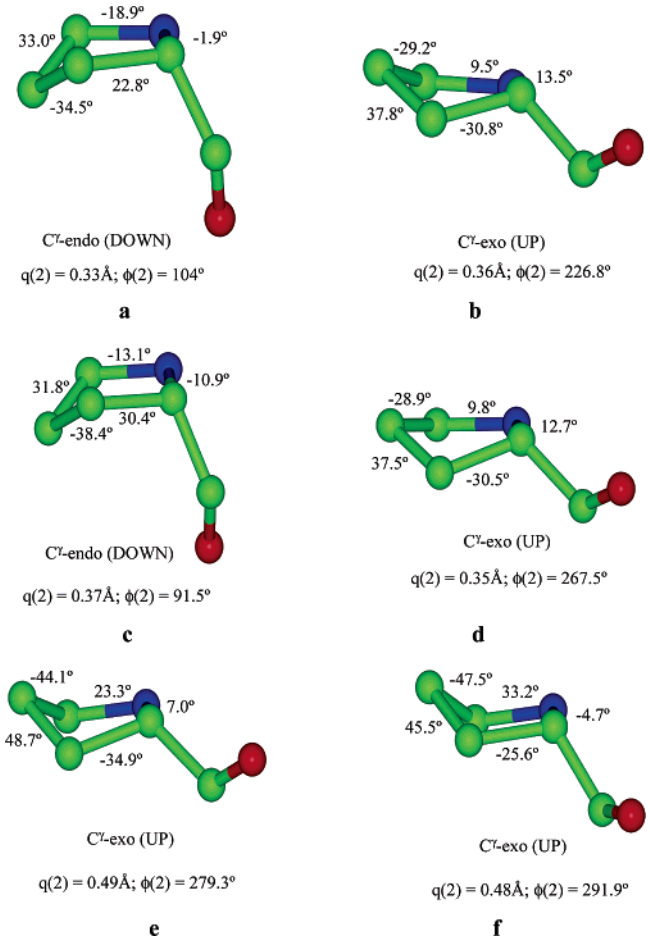

Figure 12. Proline ring puckering in the crystal structure of peptide **1** (Molecules A and B) (a−d) and an example of the helical diproline segment from the protein gingipain-R (e,f).[9] The pyrrolidine ring internal torsional angles and Cremer and Pople parameters[52] are indicated.

Pro(1) ψ requires further investigation. While recent studies have reexamined the relationship between Pro ϕ and ring pucker,[40d] reinvestigation of the effect of ring stereochemistry on Pro ψ may yield additional insights. Studies with substituted proline analogues and homologues like pipecolic acid may be of value in further defining the influence of ring conformation upon the backbone-folding properties.

Peptides **1** and **2** have provided clear evidences for the population of continuous helical conformation in solution in which the diproline segment occurs at the N-terminus of the folded structure. In both cases, the occurrence of multiple conformation in solution is clearly supported by the NMR data. In the all *trans* peptide two distinct diproline conformations α_R-α_R and P_{II}-α_R are in rapid dynamic exchange on the NMR time scale. The crystal structure of peptide **1** captures the P_{II}-α_R

(42) (a) Shi, Z.; Olson, C. A.; Rose, G. D.; Baldwin, R. L.; Kallenbach, N. R. *Proc. Natl. Acad. Sci. U.S.A.* **2002**, *99*, 9190−9195. (b) Chen, K.; Liu, Z.; Kallenbach, N. R. *Proc. Natl. Acad. Sci. U.S.A.* **2004**, *101*, 15352−15357. (c) Liu, Z.; Chen, K.; Ng, A.; Shi, Z.; Woody, R. W.; Kallenbach, N. R. *J. Am. Chem. Soc.* **2004**, *126*, 15141−15150. (d) Kentsis, A.; Mezei, M.; Gindin, T.; Osman, R. *Proteins: Struct. Funct. Bioinformatics* **2004**, *55*, 493−501. (e) Mezei, M.; Fleming, P. J.; Srinivasan, R.; Rose, G. D. *Proteins: Struct. Funct. Bioinformatics* **2004**, *55*, 502−507.

(43) (a) Pappu, R. V.; Rose, G. D. *Protein Sci.* **2002**, *11*, 2437−2455. (b) Mizuno, K.; Hayashi, T.; Peyton, D. H.; Bächinger, H. P. *J. Biol. Chem.* **2004**, *279*, 38072−38078. (c) Fleming, P. J.; Fitzkee, N. C.; Mezei, M.; Srinivasan, R.; Rose, G. D. *Protein Sci.* **2005**, *14*, 111−118. (d) Kawahara, K.; Nishi, Y.; Nakamura, S.; Uchiyama, S.; Nishiuchi, Y.; Nakazawa, T.; Ohkubo, T.; Kobayashi, Y. *Biochemistry* **2005**, *44*, 15812−15822.

(44) (a) Baldwin, R. L. *Adv. Protein Chem.* **2002**, *62*, 361−367. (b) Hodges, J. A.; Raines, R. T. *J. Am. Chem. Soc.* **2005**, *127*, 15923−15932. (c) Horng, J. C.; Raines, R. T. *Protein Sci.* **2006**, *15*, 74−83.

(45) The description of puckering in proline rings has employed variable nomenclatures. For definition of C$^\gamma$-*exo* and C$^\gamma$-*endo* form see: (a) Ramachandran, G. N.; Lakshminarayanan, A. V.; Balasubramanian, R.; Tegoni, G. *Biochim. Biophys. Acta* **1970**, *221*, 165−181. (b) Ashida, T.; Kakudo, M. *Bull. Chem. Soc. Jpn.* **1974**, *47*, 1129−1133. (c) De Tar, D. F.; Luthra, N. P. *J. Am. Chem. Soc.* **1977**, *99*, 1232−1244. For the UP and DOWN nomenclature see: Momany, F. A.; McGuire, R. E.; Burgess, A. W.; Scheraga, H. A. *J. Phys. Chem.* **1975**, *79*, 2361−2381. For recent experimental studies on the gas phase conformation of proline and hydroxyproline using Fourier transform microwave spectroscopy see: (a) Lesarri, A.; Mata, S.; Cocinero, E. J.; Blanco, S.; López, J. C.; Alonso, J. L. *Angew. Chem., Int. Ed.* **2002**, *41*, 4673−4676. (b) Lesarri, A.; Cocinero, E. J.; López, J. C.; Alonso, J. L. *J. Am. Chem. Soc.* **2005**, *127*, 2572−2579.

conformation in the solid-state. A third minor *cis* Pro-Pro conformer occurs in both peptides **1** and **2**. Interestingly, the *cis* form favors an N-terminus type VI β-turn followed by a continuous helix, which includes the second Pro residue. The observed *cis* proportions, 26% in **1** and 20% in **2**, are significantly higher than that reported for Pro-Pro segments in model sequences of Ac−Ala-Xaa-Pro-Ala-Lys-NH_2, which are water-soluble.[39b] The higher population of *cis* form in noncompetitive solvents like $CDCl_3$ may be attributed to the energetic contribution of the intramolecular hydrogen bond, in the type VI β-turn. An unusually high proportion of the Pro-Pro *cis* form was observed in a model peptide Boc-Aib-Pro-Pro-NHMe in chloroform solution in an earlier study.[20] In native protein sequences, diproline segments do occur in the α_R-α_R conformation at the N-terminus of helices. In studies of protein folding, local restrictions on the Ramachandran angles can provide a conformational bias, which can facilitate rapid folding.[46] The results described in this report support accommodation of diproline segments in the amino terminus helical turn of a short peptide helix. It remains to be definitively established whether diproline segments nucleate helical folding in a kinetic sense. Undoubtedly, both helix nucleation and stabilization will be influenced by peptide chain length and sequence effects, in addition to N-terminus capping motif. Our attempts to mimic the helix nucleating diproline conformation in a designed oligopeptide has met with some success. The success of Kemp's template is based on the covalent bridging of Pro(1) C^{γ} and Pro(2) C^{δ} by means of a thiomethylene bridge. In this tricyclic motif, Pro(1) ψ is constrained by formation of the eight membered heterocyclic ring. Coaxing an unconstrained diproline template into a favorable helix nucleating conformation may require a better understanding of the effects of flanking residues and local environmental effects on the distribution of conformer populations in Pro-Pro segments.

(46) Jha, A. K.; Colubri, A.; Zaman, M. H.; Koide, S.; Sosnick, T. R.; Freed, K. F. *Biochemistry* **2005**, *44*, 9691−9702.
(47) Gunasekaran, K. Stereochemical Analysis of Protein Structures− Lessons for Design, Engineering and Prediction, Ph. D thesis, Indian Institute of Science, Bangalore, 1997.
(48) IUPAC−IUB Commission on Biochemical Nomenclature, *Biochemistry* **1970**, *9*, 3471−3479.
(49) Fox, R. O.; Richards, F. M. *Nature (London)* **1982**, *300*, 325−330.
(50) Allen, F. H. *Acta Crystallogr.* **2002**, *B58*, 380−388.
(51) Koradi, R.; Billeter, M.; Wüthrich, K. *J. Mol. Graphics* **1996**, *14*, 51−55.
(52) Cremer, D.; Pople, J. A. *J. Am. Chem. Soc.* **1975**, *97*, 1354−1358.

Acknowledgment. We thank Prof. Stephen Hanessian for helping to obtain the crystal structure coordinates of ^{L}BcaP-^{L}Ala-^{L}Ala-OtBu (Figure 3f). This research was supported by a grant from the Council of Scientific and Industrial Research, India, and a program grant from the Department of Biotechnology, India, in the area of Molecular Diversity and Design. S. Aravinda and R. Rai thank the Council of Scientific and Industrial Research, India, and the Department of Biotechnology, India for Research Associateships. X-ray diffraction data were collected at the CCD facility funded under the IRHPA program of the Department of Science and Technology, India.

Supporting Information Available: X-ray crystallographic file for peptide **1** (cif file). The potential hydrogen bonds in peptide **1**, NMR parameters for peptide **1** in $CDCl_3$ + 10% DMSO-d_6 and DMSO-d_6. The torsion angles and hydrogen bond parameters for energy minimized crystal structure and continuous helical model. The pyrolidine ring torsion angles in proteins (for *trans*, α_R-α_R conformation) and the interproton distances for P_{II}-α_R and α_R-α_R conformation at Pro(1)-Pro(2) segment (Tables S1−S7). Molecular packing of peptide **1** in crystals (Figure S1). Structural models for peptide **2** (Figure S2). Synthetic strategy adopted for synthesis of peptides **1** and **2**, partial ROESY spectra of peptide **1** in $CDCl_3$ + 10% DMSO-d_6 and CD_3OH, partial ROESY spectra of peptide **2** in CD_3OH and $CDCl_3$ + 4.25% DMSO-d_6 and partial 700 MHz $^{1}H-^{13}C$ HSQC spectrum of peptide **1** in $CDCl_3$ at 300 K. (Figures S3−S8). This material is available free of charge via the Internet at http://pubs.acs.org.

JA060674V